Quantum-Mechanical Treatment of Inelastic Collisions. II. Exchange Reactions

DENNIS J. DIESTLER* AND VINCENT MCKOY
Gates and Crellin Laboratories of Chemistry,† California Institute of Technology, Pasadena, California
(Received 27 October 1967)

The theory for the quantum-mechanical treatment of inelastic collisions developed in the first paper of this series is extended to treat collinear, electronically adiabatic exchange reactions. The formalism is applied to three model potential energy surfaces for the exchange of identical particles. The calculated reaction probabilities are reasonable and two independent checks indicate that they are reliable.

I. INTRODUCTION

In the previous paper[1] (hereafter referred to as I) of this series we presented a new general method for the quantum-mechanical treatment of inelastic collisions of composite particles. The theory was applied to two examples of one-dimensional impulsive collisions. The purpose of this paper is to extend the theory to treat exchange reactions of the type A+BC→AB+C and then to apply the theory to several models for the exchange of identical particles, of which the simplest physically realizable example is the reaction

$$H\cdot+H_2\rightarrow H_2+H\cdot.$$

Chemical reactions constitute a special case of inelastic collisions. We wish to restrict our consideration to reactions which involve the collision of two composite particles to produce two new composite particles, i.e., *exchange reactions*. Furthermore, we shall consider only *electronically adiabatic constrained linear* encounters primarily because such a model is mathematically tractable (in contradistinction to the *nonlinear* case). Also, it is commonly assumed that the collinear path is preferred since the potential energy of interaction between an atom and a diatomic molecule is least when the atom approaches the diatomic along its line of centers. A vast amount of previous theoretical work has been devoted to this model, presumably for the same reasons. It has been treated both classically[2,3] and quantum mechanically.[4,5] Mazur and Rubin[4] solved the time-dependent Schrödinger equation for a linear model exchange reaction using a specially prepared wave packet giving directly a momentum averaged reaction probability. Unfortunately, perhaps, their potential surface was not very realistic.

Mortensen and Pitzer[5] have treated the H_2, H· exchange reaction by solving the time-independent Schrödinger equation using the Sato[6] potential surface and including "bending" corrections to take into account effects of nonlinearity. They used the finite-difference method to solve the Schrödinger equation in the inseparable region by an iterative procedure. Assuming a set of amplitudes and phases, they are able to find a solution of the finite-difference equation which deviates only slightly from the correct asymptotic solution. By analyzing the solution in the "near asymptotic" region they find a set of approximate amplitudes and phases which are "corrected to the boundary" using the WKB approximation. These corrected values are next used to obtain an improved finite-difference solution and the above procedure is repeated until convergence is obtained.

The method of treating exchange reactions which we shall develop in this paper is a straightforward extension of the treatment of inelastic collisions given in I. Briefly the method consists of building up the complete stationary wavefunction describing the reaction as a linear combination of members of a complete set of linearly independent solutions of the relevant Schrödinger equation, each member of the set also satisfying a *distinct*, yet *arbitrary*, boundary condition specified in the asymptotic region. In Sec. II the theory is extended to treat a general *collinear* exchange reaction of the form

$$A+BC\rightarrow AB+C.$$

The solution of the χ equations and the analysis of the χ_j are also discussed in Sec. II. In Sec. III we apply the theory to three model potential surfaces for the exchange of identical particles: (a) infinite-square-well surface; (b) truncated parabolic surface; (c) untruncated parabolic surface. We discuss the results and various further applications of the method now under consideration in Sec. IV.

II. EXTENSION OF THE THEORY TO EXCHANGE REACTIONS

Although the extension of the theory to exchange reactions is perhaps straightforward in principle, some simplifications can be effected by choosing an appro-

* NSF Predoctoral Fellow 1964–1967. This paper is based on part of the thesis of DJD submitted in partial fulfillment of the requirements for the degree of Doctor of Philosophy at the California Institute of Technology. Present address: Department of Chemistry, University of Missouri at St. Louis, St. Louis, Mo.

† Contribution No. 3590.

[1] D. J. Diestler and V. McKoy, J. Chem. Phys. **48**, 2941 (1968).

[2] R. De Vogelaire and M. Boudart, J. Chem. Phys. **23**, 1236 (1955).

[3] F. Wall, L. Hiller, and J. Mazur, J. Chem. Phys. **29**, 255 (1958).

[4] J. Mazur and R. Rubin, J. Chem. Phys. **31**, 1395 (1959).

[5] E. Mortensen and K. S. Pitzer, Chem. Soc. (London) Spec. Publ. No. 16, 57 (1962).

[6] S. Sato, J. Chem. Phys. **23**, 592 (1955); **23**, 2465 (1955).

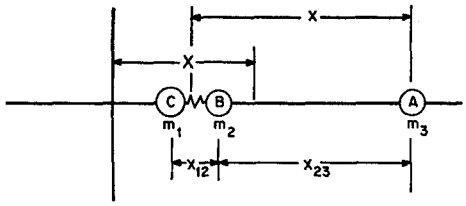

FIG. 1. Diagram of the exchange reaction A+BC→AB+C.

priate coordinate system in which to determine the χ_j's (members of the set of linearly independent solutions of Schrödinger's equation) and to analyze them into their separable components in the asymptotic region. To keep the presentation as transparent as possible we consider only a *collinear, electronically adiabatic* exchange reaction (see Fig. 1) for which the time-independent Schrödinger equation may be written as

$$\left\{-\frac{\hbar^2}{2m_1}\frac{\partial^2}{\partial x_1^2}-\frac{\hbar^2}{2m_2}\frac{\partial^2}{\partial x_2^2}-\frac{\hbar^2}{2m_3}\frac{\partial^2}{\partial x_3^2}+V_{123}\right\}\Psi=E\Psi, \quad (1)$$

where x_1, x_2, x_3 and m_1, m_2, m_3 are, respectively, the coordinates and masses of the three particles (atoms or molecular fragments) involved in the reaction. The potential V_{123} is a three-body potential, i.e., the total potential cannot be expressed as a sum of two-body interactions. This is so because, in the adiabatic approximation, the electron "clouds" of the three atoms interact with one another in a complicated fashion, adjusting instantaneously to produce an effective potential surface upon which the nuclei of the atoms move. Our task is to develop a quantum-mechanical description of the motion of these nuclei on the potential surface which will allow us to predict the probability that for a given initial state of the reactants (e.g., atom A impinging with a given initial relative velocity upon pair BC bound in a given initial eigenstate I) a reaction yielding products in some final state (e.g., atom C emerging with some final relative velocity from a newly formed pair AB bound in some final eigenstate m) will occur. Throughout this treatment we shall assume that the total energy is so low that all three particles cannot be separated, i.e., that the potential surface is such that Ψ is identically zero outside the L-shaped reaction path.

In the following treatment we shall employ four distinct coordinate systems, which are labeled $[\alpha, \beta, \gamma]$, α, β, and γ specifying the coordinates defined by a transformation. The three systems other than $[x_1, x_2, x_3]$ are defined by the following transformations:

(a) $[X, x_{12}, x_{23}]$, where

$$X=(\sum_{i=1}^{3} m_i x_i)M^{-1},$$

$$x_{12}=x_2-x_1,$$

$$x_{23}=x_3-x_2;$$

(b) $[X, x, x_{12}]$, where

$$X=(\sum_{i=1}^{3} m_i x_i)M^{-1},$$

$$x=x_3-(m_1x_1+m_2x_2)(m_1+m_2)^{-1},$$

$$x_{12}=x_2-x_1;$$

(c) $[X, x', x_{23}]$, where

$$X=(\sum_{i=1}^{3} m_i x_i)M^{-1},$$

$$x'=x_1-(m_2x_2+m_3x_3)(m_2+m_3)^{-1},$$

$$x_{23}=x_3-x_2.$$

In these equations the symbols have their usual significance, i.e., x_1, x_2, x_3 are the particle coordinates in an arbitrary space-fixed reference frame, X is the coordinate of the center of mass in this frame, x_{12} and x_{23} are the interparticle separations, and x and x' are the coordinates of particles A (3) and C (1), respectively, with respect to the center of mass of the bound pair. Since the potential V_{123} is independent of X, we can separate out the center-of-mass motion in each of the three coordinate systems defined above. Hence,

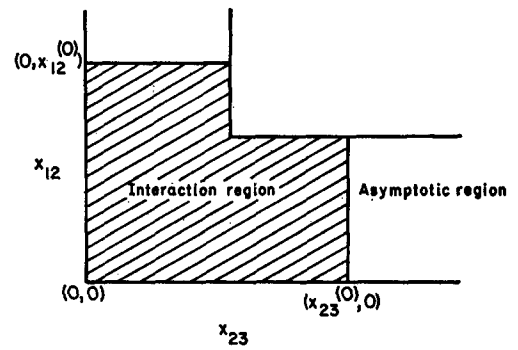

(a)

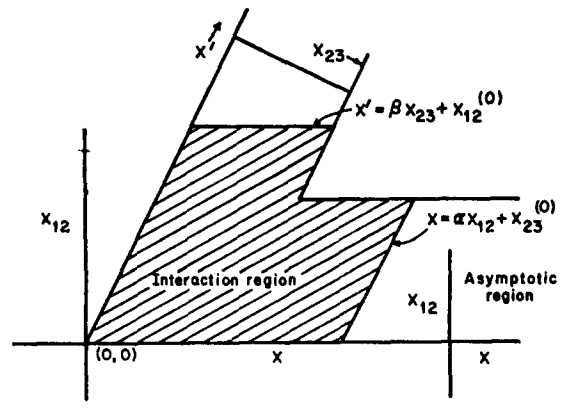

(b)

FIG. 2. Coordinate systems used in the treatment of exchange reactions showing boundary conditions and interaction region: (a) $[X, x_{12}, x_{23}]$, (b) $[X, x, x_{12}]$ and $[X, x', x_{23}]$.

in $[X, x_{12}, x_{23}]$ the Schrödinger equation for the relative motion becomes

$$\left\{-\frac{\hbar^2}{2\mu_{12}}\frac{\partial^2}{\partial x_{12}^2}-\frac{\hbar^2}{2\mu_{23}}\frac{\partial^2}{\partial x_{23}^2}+\frac{\hbar^2}{m_2}\frac{\partial^2}{\partial x_{12}\partial x_{23}}+V_{123}\right\}\psi=E_r\psi, \quad (2)$$

where

$$\mu_{ij}=m_im_j(m_i+m_j)^{-1}.$$

The coordinate system showing the interaction region and boundary conditions is sketched in Fig. 2(a). We shall assume that each bound pair has a discrete eigenvalue spectrum and that $V_{123}=V_{12}$ for $x_{23}>x_{23}^{(0)}$, $V_{123}=V_{23}$ for $x_{12}>x_{12}^{(0)}$. These "cutoff" parameters define the inseparable region in a manner analogous to x_0 and x_0' for the case of nonreactive collisions.[1] We also sketch [see Fig. 2(b)] the boundary conditions and inseparable region in the systems $[X, x, x_{12}]$ and $[X, x', x_{23}]$ since the asymptotic forms of ψ assume a simpler, more pleasing appearance than in $[X, x_{12}, x_{23}]$.

We now wish to find a total wavefunction ψ satisfying the wave Eq. (2) everywhere and having the following asymptotic forms in $[X, x, x_{12}]$ and $[X, x', x_{23}]$:

Equations (3) can now be expressed as

$$\psi(x, x_{12})=\exp(-ik_Ix)\phi_I(x_{12})+\sum_{m=1}^{N}R_m\exp(ik_mx)\phi m(x_{12})+\mathcal{O}[\exp(-\gamma x)], \qquad x\geq x_0=\alpha x_{12}+x_{23}^{(0)}, \quad (3a)$$

$$\psi(x', x_{23})=\sum_{m=1}^{N'}T_m\exp(ik'_mx')\bar{\phi}_m(x_{23})+\mathcal{O}[\exp(-\gamma x')], \qquad x'\geq x_0'=\beta x_{23}+x_{12}^{(0)}, \quad (3b)$$

where

$$\alpha=m_1(m_1+m_2)^{-1},$$
$$\beta=m_3(m_2+m_3)^{-1},$$

and ϕ_m and $\bar{\phi}_m$ are the bound-state eigenfunctions of the BC and AB subsystems, respectively, and the exponentials are the corresponding free-particle wavefunctions. The energy-conservation condition may be expressed as

$$\begin{aligned}E_r&=\epsilon_{12}^{(I)}+(\hbar^2k_I^2/2\mu_{12,3})\\&=\epsilon_{12}^{(m)}+(\hbar^2k_m^2/2\mu_{12,3})\\&=\epsilon_{23}^{(m)}+(\hbar^2k_m'^2/2\mu_{23,1}),\end{aligned} \quad (4)$$

where $\mu_{ij,k}=(m_i+m_j)m_k(m_i+m_j+m_k)^{-1}$ and $\epsilon_{ij}^{(m)}$ is the energy eigenvalue associated with the mth eigenstate of the ij pair. We may interpret the asymptotic behavior of ψ as given in Eqs. (3) analogously to that of the wavefunction describing a nonreactive collision as discussed in Paper I, i.e., the total scattering (reaction) consists of an incident wave of unit amplitude in channel I plus scattered waves of various amplitudes corresponding to reaction and also reflection *without* reaction. Thus R_m is the amplitude for excitation of the initially bound pair BC from state I to m and reflection of A with momentum $\hbar k_m$ relative to the center of mass of BC. T_m is the amplitude for reaction to occur, producing bound pair AB in state m and ejecting C with momentum $\hbar k_m'$ relative to the center of mass of AB. The transition probabilities are given by

$$P_{I\to m}^{(R)}=(k_m/k_I)\mid R_m\mid^2, \quad (5a)$$

$$P_{I\to m}^{(T)}=(k_m'/k_I)\mid T_m\mid^2, \quad (5b)$$

where $P_{I\to m}^{(R)}$ is the probability that the incoming particle A will excite (or de-excite) subsystem BC from incident state I to final state m and reflect, $P_{I\to m}^{(T)}$ is the probability that A will react with subsystem BC in state I to form a new subsystem AB in state m, ejecting C.

Current conservation, which requires that

$$\sum_{m=1}^{N}\frac{k_m}{k_I}\mid R_m\mid^2+\sum_{m=1}^{N'}\frac{k_m'}{k_I}\mid T_m\mid^2=1, \quad (6)$$

again provides a useful check on the accuracy of numerical computation of the transition probabilities. The following relation holds for general exchange reactions by time-reversal invariance:

$$P_{i\to j}^{(R)}=P_{j\to i}^{(R)}. \quad (7a)$$

For the exchange of *identical* particles we also have

$$P_{i\to j}^{(T)}=P_{j\to i}^{(T)}. \quad (7b)$$

As in the case of nonreactive collisions, our primary goal is to obtain the R's and T's and we accomplish this again by finding the appropriate linear combination of linearly independent χ_j's, each χ_j satisfying the Schrödinger equation (2) in addition to *arbitrary* boundary conditions specified in the asymptotic regions. In $[X, x_{12}, x_{23}]$, each χ_j has the asymptotic form

$$\chi_j=\sum_{l=1}^{N}\{A_l^{(j)}\exp[-ik_l(\alpha x_{12}+x_{23})]+\bar{A}_l^{(j)}\exp[ik_l(\alpha x_{12}+x_{23})]\}\phi_l(x_{12})$$
$$+\sum_{l>N}\{B_l^{(j)}\exp[-k_l(\alpha x_{12}+x_{23})]+\bar{B}_l^{(j)}\exp[k_l(\alpha x_{12}+x_{23})]\}\phi_l(x_{12}), \qquad x_{23}\geq x_{23}^{(0)}, \quad (8a)$$

$$\chi_j=\sum_{l=1}^{N'}\{\alpha_l^{(j)}\exp[-ik_l'(\beta x_{23}+x_{12})]+\bar{\alpha}_l^{(j)}\exp[ik_l'(\beta x_{23}+x_{12})]\}\bar{\phi}_l(x_{23})$$
$$+\sum_{l>N'}\{\beta_l^{(j)}\exp[-k_l'(\beta x_{23}+x_{12})]+\bar{\beta}_l^{(j)}\exp[k_l'(\beta x_{23}+x_{12})]\}\bar{\phi}_l(x_{23}), \qquad x_{12}\geq x_{12}^{(0)}, \quad (8b)$$

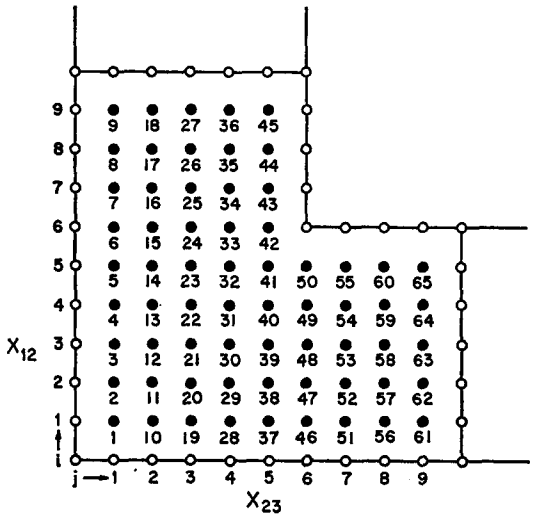

FIG. 3. Finite-difference mesh used in the treatment of exchange reactions in the coordinate system $[X, x_{12}, x_{23}]$.

where N and N' are the number of *open* channels for subsystems BC and AB, respectively, and where the energy conservation relation (4) holds. The χ_j, as given by Eqs. (8), satisfies the wave equation (2) in the asymptotic regions. We may interpret the right member of Eq. (8a) as an expansion of χ_j in the "complete" orthonormal set of eigenfunctions of the Hamiltonian with $V_{123}\rightarrow V_{23}(x_{23})$. Similarly, the right number of Eq. (8b) is an expansion of χ_j (in the other asymptotic region) in the "complete" orthonormal set of eigenfunctions of the Hamiltonian with $V_{123}\rightarrow V_{12}(x_{12})$. "Complete" here is used in the same sense as in I, i.e., *any* function χ satisfying Eq. (2) may be expanded as in Eqs. (8).

The total wavefunction for the reaction may now be written as

$$\psi=\sum_{j=1}^{\infty} c_j^{(I)}\chi_j, \tag{9}$$

such that ψ is everywhere a solution of Eq. (2) and has the proper asymptotic form [Eqs. (8)]. Hence, we must require that

$$\sum_j c_j^{(I)}A_l^{(j)}=\delta_{Il}, \qquad l\leq N, \tag{10a}$$

$$\sum_j c_j^{(I)}\bar{B}_l^{(j)}=0, \qquad l>N, \tag{10b}$$

$$\sum_j c_j^{(I)}\alpha_l^{(j)}=0, \qquad l\leq N', \tag{10c}$$

$$\sum_j c_j^{(I)}\bar{\beta}_l^{(j)}=0, \qquad l>N', \tag{10d}$$

where the superscript I on $c_j^{(I)}$ denotes the incident state. The physical interpretation of these equations is as follows: Equation (10a) corresponds to the requirement that we have a monoenergetic beam of particles C incident from the left; Eq. (10c) to the fact that there are no particles A incident from the right; Eqs. (10b) and (10d) eliminate the *rising* virtual components in regions $x_{23}\geq x_{23}^{(0)}$ and $x_{12}\geq x_{12}^{(0)}$, respectively. Truncating the expansions in l and j, we obtain a finite system of linear equations expressed in matrix form as

$$\mathbf{AC}=\mathbf{I}', \tag{11}$$

where $\mathbf{A}$ is the $(M+M')\times(M+M')$ matrix of coefficients $A_l^{(j)}$, $\bar{B}_l^{(j)}$, etc., $\mathbf{C}$ is the $(M+M')\times N$ matrix of $c_j^{(I)}$, and $\mathbf{I}'$ is the $(M+M')\times N$ matrix consisting of a $N\times N$ unit matrix occupying the first N rows and a $(M+M'-N)\times N$ null matrix the remaining rows. M is the total number of BC channels and M' the total number of AB channels retained in the truncated state expansion (9). The amplitudes R_m and T_m are determined from

$$\boldsymbol{\tau}\equiv\bar{\mathbf{A}}\mathbf{C}=\bar{\mathbf{A}}\mathbf{A}^{-1}\mathbf{I}', \tag{12}$$

where $\bar{\mathbf{A}}$ is the $(N+N')\times(M+M')$ matrix of coefficients $\bar{A}_l^{(j)}$ and $\bar{\alpha}_l^{(j)}$, $\mathbf{C}$ is the matrix of $c_j^{(I)}$ determined from Eq. (11), and $\boldsymbol{\tau}$ is the $(N+N')\times N$ matrix, the first N rows of which are the R_m, the next N' the T_m.

Determination of the χ_j

The χ may be determined most easily by the finite-difference method in the coordinate system $[X, x_{12}, x_{23}]$. Making the substitutions[7]

$$(\partial^2/\partial x_{12}^2)_{i,j}=(1/h^2)(\chi_{i+1,j}-2\chi_{i,j}+\chi_{i-1,j})+\mathcal{O}(h^2), \tag{13a}$$

$$(\partial^2/\partial x_{23}^2)_{i,j}=(1/h^2)(\chi_{i,j+1}-2\chi_{i,j}+\chi_{i,j-1})+\mathcal{O}(h^2), \tag{13b}$$

$$(\partial^2/\partial x_{12}\partial x_{23})_{i,j}=(1/4h^2)(\chi_{i+1,j+1}-\chi_{i+1,j-1}-\chi_{i-1,j+1}+\chi_{i-1,j-1})+\mathcal{O}(h^2), \tag{13c}$$

we obtain for the discretized Schrödinger equation (2)

$$-\mu_{12}^{-1}(\chi_{i,j-1}+\chi_{i,j+1})-\mu_{23}^{-1}(\chi_{i-1,j}+\chi_{i+1,j})+(2m_2)^{-1}(\chi_{i-1,j-1}-\chi_{i-1,j+1}-\chi_{i+1,j-1}+\chi_{i+1,j+1})$$
$$+2[\mu_{12}^{-1}+\mu_{23}^{-1}+\hbar^{-2}(\{V_{123}\}_{i,j}-E_r)h^2]\chi_{i,j}=0, \tag{14}$$

where h is the mesh size and the indices i and j denote the particular point of the mesh as shown in Fig. 3.

[7] M. Abramowitz and I. Stegun, Natl. Bur. Appl. Math. Ser. No. 55, 884 (1964).

The subscript j of χ_j, denoting the jth member of the linearly independent set, has been dropped. We note that even though the Hamiltonian contains a mixed partial derivative in the kinetic term, this is not difficult to incorporate into the finite-difference equations and does not ruin the symmetry or "bandedness" of the finite-difference matrix. The bandwidth, however, is greater than that of a matrix corresponding to a nonreactive collision. This is evident from a comparison of the meshes used in the two cases. Furthermore, the boundary conditions are separable in $[X, x_{12}, x_{23}]$ and it is easy to construct a uniform mesh, as we have seen in Fig. 3.

It is possible to make arguments about uniqueness and convergence analogous to those given in I. We shall not review these here. The infinite-difference equations are solved using the McCormick computer subroutine, which is discussed in detail in I.

Analysis of the χ_j

As an example of the procedure we consider the determination of the coefficients $A_l^{(j)}$, $\bar{A}_l^{(j)}$, $B_l^{(j)}$, and $\bar{B}_l^{(j)}$ of the components in the asymptotic form [Eq. (8a)]. Multiplying Eq. (8a) by ϕ_m^* and integrating with respect to x_{12} over all space, we obtain the following equation:

$$\sum_{l=1}^{N}[I_{ml}(x_{23})A_l^{(j)}+I_{ml}^*\bar{A}_l^{(j)}]+\sum_{l>N}[H_{ml}(x_{23})B_m^{(j)}+G_{ml}(x_{23})\bar{B}_m^{(j)}]=g_m^{(j)}(x_{23}),\qquad m=1, 2, 3, \cdots, \tag{15}$$

where

$$I_{ml}=\int_{-\infty}^{\infty}\phi_m^*(x_{12})\phi_l(x_{12})\exp(-ik_l\alpha x_{12})\,dx_{12}\exp(-ik_l x_{23}), \tag{16a}$$

$$H_{ml}=\int_{-\infty}^{\infty}\phi_m^*(x_{12})\phi_l(x_{12})\exp(-k_l\alpha x_{12})\,dx_{12}\exp(-k_l x_{23}), \tag{16b}$$

$$G_{ml}=\int_{-\infty}^{\infty}\phi_m^*(x_{12})\phi_l(x_{12})\exp(k_l\alpha x_{12})\,dx_{12}\exp(k_l x_{23}), \tag{16c}$$

and

$$g_m^{(j)}(x_{23})=\int_{-\infty}^{\infty}\phi_m^*(x_{12})\chi_j(x_{12}, x_{23})\,dx_{12}. \tag{16d}$$

We note that Eq. (15) is, in fact, a set of simultaneous equations involving all the unknown coefficients. We solve this set of equations by truncating the expansion in l and taking a finite number of inner products m, adding successively more terms until convergence of the coefficients is achieved. If we retain L terms in the l expansion, then we have L equations (obtained by taking inner products with ϕ_m, $m=1, 2, 3, \cdots, L$) in $2L$ unknowns, there being an "unbarred" and "barred" coefficient for each of the L components retained. Hence, we secure two equations for each value of m by choosing two different values of $x_{23}\geq x_{23}^{(0)}$. Thus we obtain a system of $2L$ simultaneous equations in $2L$ unknowns. We call the associated matrix of coefficients of unknowns the *analysis matrix*. A similar analysis of χ_j for $\alpha_l^{(j)}$, $\bar{\alpha}_l^{(j)}$, etc. may be carried out in the other asymptotic region.

For the model exchange reactions treated in Sec. III we have found it necessary to take L equal to five or six (using a computer subroutine which solves systems of equations with complex coefficients) for a four-channel (two open, two virtual) state expansion of χ_j. Analyses seem to be more sensitive to the choice of the pair of x_{23} values than in the analysis of χ_j's for nonreactive collisions. Of course, if the values lie very near one another, the analysis matrix is nearly singular. Hence, we choose pairs of values that are as far apart as possible in the asymptotic regions. We shall discuss this problem in greater detail below.

The integrals $g_m^{(j)}$ are evaluated numerically using the extended Simpson's rule discussed in I.

III. APPLICATION OF THE THEORY TO EXCHANGE REACTIONS INVOLVING EQUIVALENT PARTICLES

In this section we consider three models for the exchange reaction involving three *equivalent* particles. Though the particles are equivalent, they are not *indistinguishable* since they cannot penetrate one another. We solve for the χ_j in $[X, x_{12}, x_{23}]$. Since V_{123} is symmetric about $x_{12}=x_{23}$, it is necessary to solve for only half as many χ_j's as usual. Suppose we include $M(=M')$ channels in the truncated state expansion. Then, according to the development in Sec. II, we need $2M$ linearly independent χ_j's. We find M of these using the following set of boundary conditions: $\chi_j(x_{12}, x_{23}\geq x_{23}^{(0)})=\phi_j(x_{12})$, $\chi_j(x_{12}\geq x_{12}^{(0)}, x_{23})\equiv 0$, $j=1, 2, \cdots, M$. To determine the remaining M χ_j's we simply use the "reversed" set of

TABLE I. Transition probabilities as a function of mesh size for square-well potential surface ($a=\pi$; $E'=2.125$; number of virtual channels=2).

Mesh size	$P_{1\to1}^{(R)}$	$P_{1\to2}^{(R)}$	$P_{1\to1}^{(T)}$	$P_{1\to2}^{(T)}$	$\prod_{T,R,i=1}^{2} P_{1\to i}$
0.1571	0.7673	0.0249	0.1178	0.0859	0.9959
0.1308	0.7590	0.0267	0.1208	0.0911	0.9976
0.1122	0.7539	0.0279	0.1225	0.0943	0.9986
0.0982	0.7509	0.0286	0.1237	0.0965	0.9997
Extrapolated value	0.7404	0.0306	0.1264	0.1042	1.0016
	$P_{2\to1}^{(R)}$	$P_{2\to2}^{(R)}$	$P_{2\to1}^{(T)}$	$P_{2\to2}^{(T)}$	$\sum_{T,R,i=1}^{2} P_{2\to i}$
0.1571	0.0251	0.4398	0.0942	0.4453	1.0054
0.1308	0.0268	0.4429	0.0960	0.4369	1.0026
0.1122	0.0278	0.4451	0.0971	0.4314	1.0014
0.0982	0.0284	0.4466	0.0978	0.4277	1.0005
Extrapolated value	0.0300	0.4562	0.1014	0.4116	0.9992

conditions: $\chi_j(x_{12}, x_{23}\geq x_{23}^{(0)})\equiv 0$, $\chi_j(x_{12}\geq x_{12}^{(0)}, x_{23})=\phi_j$, $j=1, 2, \cdots, M$. But the χ_j's corresponding to the reversed set of conditions are identical to the first M χ_j's reflected about the line $x_{12}-x_{23}=0$. Hence, it is necessary to determine only M χ_j's, i.e., to solve the finite-difference equations only M times. We have done this for several model potential surfaces.

A. Infinite-Square-Well Potential Surface

We consider first the simplest possible potential surface, i.e., $V_{123}\equiv 0$ inside the L-shaped reaction path and $V_{123}=\infty$ outside. Thus, each subsystem is bound by an infinite-square-well potential. Making the substitutions

$$x_{12}=(a/\pi)x_{12}',$$
$$x_{23}=(a/\pi)x_{23}'$$

in Eq. (2) and then multiplying both members by $(\hbar^2\pi^2/\mu_{12}a^2)^{-1}$, we obtain

$$\left\{-\frac{1}{2}\frac{\partial^2}{\partial x_{12}'^2}-\frac{1}{2}\frac{\partial^2}{\partial x_{23}'^2}+\frac{1}{(m_2/\mu_{12})}\frac{\partial^2}{\partial x_{12}\partial x_{23}}\right\}\psi=E'\psi, \quad (17)$$

where

$$E'=(\mu_{12}a^2/\hbar^2\pi^2)E_r.$$

The eigenvalue spectra of the two subsystems are discrete, the eigenfunctions and eigenvalues being given by

$$\phi_n(x_{12})=(2/\pi)^{1/2}\sin nx_{12}',$$
$$\epsilon_{12}^{(n)}=n^2/2,$$

respectively, for the BC subsystem. Energy conservation requires, as usual,

$$E'=(n^2/2)+(\mu_{12}a^2k_n^2/2\pi^2\mu_{12,3}),$$

where k_n is the free-particle wavenumber. Since the particles are identical, we have $m_2/\mu_{12}=2$, $\mu_{12}/\mu_{12,3}=\frac{3}{4}$. Transition probabilities have been determined for $E'=2.125$ (two open channels), $a=\pi$, $x_{12}^{(0)}=x_{23}^{(0)}=\pi$. It was necessary to retain only two virtual channels in the state expansion and five for the analysis of χ_j. Transition probabilities as a function of mesh size are given in Table I along with Richardson-extrapolated values.[8] Since probabilities for only four different mesh sizes were obtained, an accurate e_1^m extrapolation[8] was not possible.

From Table I we observe that current-sum and time-reversal checks are good not only for individual mesh values but also, as expected, for the extrapolated values. For example, $P_{1\to2}^{(R)}$ and $P_{2\to1}^{(R)}$ differ by less than 2% (0.006) and $P_{1\to2}^{(T)}$ and $P_{2\to1}^{(T)}$ by less than 3% (0.0028).

B. Truncated Parabolic Potential Surface

A more realistic potential surface is described by the expressions

$$V_{123}=\tfrac{1}{2}\kappa(x_{12}-x_{120})^2, \quad x_{23}>x_{23}^{(0)}, \quad 0\leq x_{12}\leq a,$$
$$V_{123}=\infty, \quad x_{23}>x_{23}^{(0)}, \quad x_{12}<0, \quad x_{12}>a; \quad (18a)$$
$$V_{123}=\tfrac{1}{2}\kappa\{[(2x_{120}-x_{12})^2+(2x_{230}-x_{23})^2]^{1/2}-x_{120}\}^2, \quad x_{12}\leq x_{12}^{(0)}, \quad x_{23}\leq x_{23}^{(0)};$$
$$V_{123}=\infty, \quad x_{12}, \quad x_{23}<0, \quad (18b)$$
$$V_{123}=\tfrac{1}{2}\kappa(x_{23}-x_{230})^2, \quad x_{12}>x_{12}^{(0)}, \quad 0\leq x_{23}\leq a,$$
$$V_{123}=\infty, \quad x_{12}>x_{12}^{(0)}, \quad x_{23}<0, \quad x_{23}>a, \quad (18c)$$

where $x_{120}=x_{230}$, the equilibrium separation of the two particles in the equivalent subsystems. The potential surface described by Eqs. (18) is sketched in Fig. 4. In the asymptotic regions the potential surface is a *truncated* parabolic cylinder. In the interaction region it is a curved parabolic cylinder generated by rotating a parabola centered at $x_{120}=x_{230}$ about an axis at ($x_{12}=2x_{120}$, $x_{23}=2x_{230}$) perpendicular to the x_{12}-x_{23}

[8] See paper I of this series (preceding paper).

plane. With the substitutions

$$x_{12}'=(\pi/a)x_{12},$$

$$x_{23}'=(\pi/a)x_{23},$$

the Schrödinger equation (2) becomes

$$\left\{-\frac{1}{2}\frac{\partial^2}{\partial x_{12}'^2}-\frac{1}{2}\frac{\partial^2}{\partial x_{23}'^2}+\frac{1}{2\gamma}\frac{\partial^2}{\partial x_{12}'\partial x_{23}'}+V_{123}'\right\}\psi=E'\psi, \quad (19)$$

where

$$\gamma=m_2/2\mu_{12},$$

$$V_{123}'=(\hbar^2\pi^2/\mu_{12}a^2)^{-1}V_{123},$$

$$E'=(\hbar^2\pi^2/\mu_{12}a^2)^{-1}E_r,$$

and a is the well width, i.e., the truncation point. The eigenvalues and eigenfunctions of the truncated parabolic binding potential are determined using the Ritz linear variational method, expressing the trial function as a linear combination of "particle-in-a-box" eigenfunctions as

$$\phi_k(x_{12}')=\left(\frac{2}{\pi}\right)^{1/2}\sum_{n=1}^{n_{\max}}c_{kn}\sin nx_{12}'. \quad (20)$$

Energy conservation requires

$$(E_{\mathrm{KE}})_n+\epsilon_{12}^{(n)}=E',$$

where $\epsilon_{12}^{(n)}$ is the approximate eigenvalue associated with the nth eigenstate and $(E_{\mathrm{KE}})_n$ is the corresponding energy of the free particle, either A or C. Since we are dealing with identical particles the mass ratios are fixed as follows: $\mu_{12}=\frac{1}{2}$, $\gamma=1$. Transition probabilities are given in Table II for other system parameters arbitrarily fixed as follows: $\kappa=10.0$; $a=\pi$; $x_{120}=\pi/2$; $E'=5.0$; $n_{\max}=10$. For this particular energy there are two open channels; it was found sufficient to retain three virtual channels in the state expansions. We retained five or six states in the χ_j analysis, taking values of x_{12}' (or x_{23}') as far apart as possible in the asymptotic regions. As one can see from Table II, the values converge in a regular fashion, with current-sum and time-reversal checks improving as the mesh size decreases. Probabilities obtained by doing the χ_j analyses at values of x_{12}' (or x_{23}') closer together differ little (less than 1%) from the values of Table II. Also, including more eigenfunctions in the variational trial function Eq. (20), i.e., taking $n_{\max}>10$, induces an insignificant change in the transition probabilities.

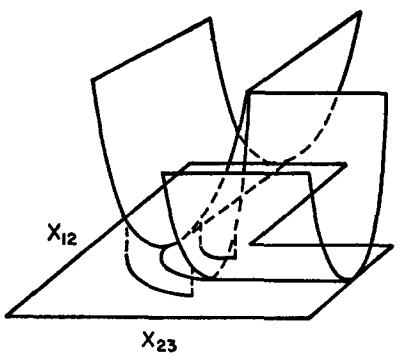

FIG. 4. Sketch of truncated parabolic surface for model exchange reaction.

TABLE II. Transition probabilities as a function of mesh size for truncated parabolic surface ($\kappa=10.0$; $E'=5.0$; $a=\pi$; number of virtual channels=3).

Mesh size	$P_{1\to1}^{(R)}$	$P_{1\to2}^{(R)}$	$P_{1\to1}^{(T)}$	$P_{1\to2}^{(T)}$	$\sum_{T,R,i=1}^{2}P_{1\to i}$
0.1571	0.0455	0.1134	0.6489	0.1774	0.9852
0.1308	0.0538	0.1196	0.6327	0.1832	0.9893
0.1122	0.0595	0.1233	0.6224	0.1865	0.9917
0.0982	0.0635	0.1256	0.6156	0.1885	0.9932
Extrapolated value	0.0779	0.1326	0.5932	0.1939	0.9976
	$P_{2\to1}^{(R)}$	$P_{2\to2}^{(R)}$	$P_{2\to1}^{(T)}$	$P_{2\to2}^{(T)}$	$\sum_{T,R,i=1}^{2}P_{2\to i}$
0.1571	0.1178	0.4271	0.2048	0.2673	1.0170
0.1308	0.1230	0.4177	0.2022	0.2688	1.0117
0.1122	0.1262	0.4118	0.2007	0.2701	1.0088
0.0982	0.1282	0.4079	0.1997	0.2712	1.0070
Extrapolated value	0.1347	0.3958	0.1958	0.2753	1.0016

C. Untruncated Parabolic Surface

Certainly a more realistic potential surface is that described by Eqs. (18) without the truncation. In this case the binding potentials become "pure" parabolic in the asymptotic regions. In order to determine the χ_j we take the interaction region to be large enough that the χ_j are negligibly small outside the L-shaped reaction path, requiring that $\chi_j\equiv0$ outside the region. Making the substitutions

$$\xi'=(\hbar^2/\mu_{12}\omega)^{-1/2}x_{12},$$

$$\xi=(\hbar^2/\mu_{12}\omega)^{-1/2}x_{23},$$

we obtain for the wave equation (2)

$$\left\{-\frac{1}{2}\frac{\partial^2}{\partial\xi'^2}-\frac{1}{2}\frac{\partial^2}{\partial\xi^2}+\frac{1}{2\gamma}\frac{\partial^2}{\partial\xi\partial\xi'}+V_{123}'\right\}\psi=E'\psi, \quad (21)$$

where

$$\gamma=m_2/2\mu_{12},$$

$$E'=E_r/\hbar\omega,$$

$$V_{123}'=V_{123}/\hbar\omega,$$

$$\omega=(\kappa/\mu_{12})^{1/2}.$$

The eigenfunctions and eigenvalues of the subsystem

TABLE III. Transition probabilities for the untruncated parabolic surface ($a=10.0$; $E'=1.75$; $h=0.4165$; number of virtual channels=2). The columns correspond to various analyses of χ_i as discussed in the text.

Transition probability	1	2	3	4
$P_{1\to1}^{(R)}$	0.000667	0.000611	0.000915	0.00103
$P_{1\to2}^{(R)}$	0.003135	0.002430	0.001429	0.00840
$P_{1\to1}^{(T)}$	0.724909	0.712349	0.698335	0.68557
$P_{1\to2}^{(T)}$	0.256870	0.283050	0.314947	0.34546
$\sum_{R,T,i=1}^{2} P_{1\to i}$	0.995581	0.998440	1.015626	1.04146
$P_{2\to1}^{(R)}$	0.000306	0.001567	0.002316	0.00268
$P_{2\to2}^{(R)}$	0.005751	0.005947	0.004405	0.00277
$P_{2\to1}^{(T)}$	0.292969	0.287198	0.283838	0.28214
$P_{2\to2}^{(T)}$	0.719046	0.707013	0.694846	0.68384
$\sum_{R,T,i=1}^{2} P_{2\to i}$	1.018072	1.001725	0.985405	0.97143

bound states are given by

$$\phi_n(\xi)=(2^n n!\pi^{1/2})^{-1/2}H_n(\xi)\exp(-\xi^2/2),$$

$$\epsilon_{12}^{(n)}=(n+\tfrac{1}{2}),$$

which are just the eigenfunctions and eigenvalues of a harmonic oscillator having a classical frequency ω. Energy conservation gives

$$(E_{\mathrm{KE}})_n+(n+\tfrac{1}{2})=E',$$

where $(E_{\mathrm{KE}})_n$ is the kinetic energy of the free particle, A or C. Since we are assuming that all three particles are identical, mass ratios are fixed at: $\mu_{12}=\frac{1}{2}$; $\gamma=1$.

In treating the problem using the parameters $a=10.0$, $E'=1.75$ (two open channels), difficulties arose. The problem is summarized in Table III, which lists transition probabilities obtained using a mesh size of 0.4165 ($n_w=23$, number of points across the well) and two virtual channels in the state expansion. This is quite a crude mesh and the difficulties, mentioned below, are not quite unexpected. For this mesh size there are four pairs of values of ξ (or ξ') for which the analysis of χ_j may be carried out. Probabilities obtained using these various possible pairs are listed in the columns of Table III. The first column corresponds to the ξ (or ξ') values farthest apart, the second to next closest values, and so on. Clearly the various sets of probabilities differ significantly. Column 2 seems to best satisfy the current-sum and time-reversal checks, although there is no obvious reason that this should be true. These discrepancies are due to the very crude mesh we have used. For example, the finest mesh attainable for $a=10.0$ corresponds to $h=0.325$, to be compared with $h=0.157$ for the coarsest mesh used in the treatment of the truncated parabolic surface. We can certainly expect an improvement using finer meshes. We have not done this because there are alternative ways of removing these discrepancies. These should be more generally applicable and are discussed in the next section. Inclusion of more virtual channels in either the state expansion or the χ_j analysis did not alter the columns of Table III before the fifth decimal place. Although there is no sound reason to favor the second column, we would expect the third and fourth columns to be more in error since the analysis matrix may be ill-conditioned for ξ values too near one another.

IV. DISCUSSION

By a rather simple extension of the general method for the treatment of inelastic collisions presented in I, we have been able to treat an important special class of chemical reactions—exchange reactions. We have obtained very reasonable and self-consistent results for the reaction probabilities on several model potential surfaces for constrained linear, electronically adiabatic encounters. The crucial feature of our method is that it avoids the difficulty of the usual state expansion

$$\psi=\sum_k f_k\phi_k, \tag{22}$$

where ϕ_k are eigenfunctions of the initially bound pair BC and f_k are arbitrary functions of the coordinate of the incoming particle A relative to the center of mass of BC. The difficulty is that the bound state functions ϕ_k do not form a complete set over the whole reaction space and hence ψ cannot be everywhere expressed as in Eq. (22). In our method it is not necessary to expand the functions χ_j in any particular set, except in either asymptotic region where expansions (8) are valid.

From our results on the untruncated parabolic potential surface, it is clear that very coarse meshes, which appear useful for large interaction regions, may give rise to a type of "instability" or inconsistency in treating exchange reactions by the finite-difference method. If we insist on solving the χ equations by finite differences there are three possible ways of circumventing this "instability" caused by coarse meshes in large interaction regions. First, one can simply go to smaller meshes. The number of equations will increase but these can still be solved using our present computer programs. This is the simplest way of improving the results. Second, we can use a smaller interaction region, specifying the boundary condition in the "near-asymptotic" region and then extending the solution into the asymptotic region by the WKB method (assuming the potential is essentially separable in the "near-asymptotic" region). Third, for exchange reactions involving identical particles, we can split the reaction path into two parts by the line $x_{12}=x_{23}$ and

then solve for odd and even χ_j, requiring χ_j to vanish on $x_{12}=x_{23}$ for the odd functions and $\nabla\chi_j$ to vanish on $x_{12}=x_{23}$ for even functions. Although this procedure reduces by a factor of 2 the dimension of the finite-difference matrix and also the bandwidth, it gives rise to an unsymmetric matrix for the even solutions. However, we can symmetrize the matrix by multiplying by its transpose, thereby doubling the bandwidth. We are investigating both of these latter alternative methods for dealing with large interaction regions.

A very useful application of our method would be an investigation of a parametrized potential surface to determine the regions of the surface to which reaction probabilities are most sensitive for a given incident total energy and also how the relative distribution of total energy between vibrational and translational degrees of freedom affects reaction probabilities. Such a parametrized surface has been studied classically by Wall and Porter.[9] It should be of interest to compare our quantum-mechanical results with the classical results and with quantum-mechanical approximations. This comparison can give us an idea of the importance of quantum effects and the conditions under which these other approximations are reliable.

[9] F. Wall and R. Porter, J. Chem. Phys. **36**, 3256 (1962); **39**, 3112 (1963).

THE JOURNAL OF CHEMICAL PHYSICS VOLUME 48, NUMBER 7 1 APRIL 1968

Infrared Matrix-Isolation Studies of Nuclear-Spin-Species Conversion*

H. P. Hopkins, Jr.,† R. F. Curl, Jr., and Kenneth S. Pitzer

Chemistry Department, Rice University, Houston, Texas

(Received 10 October 1967)

Studies of the time evolution of intensities in the fine structure of infrared bands of CH_3D, H_2O, and NH_3 isolated in rare-gas matrices in the temperature region 6.5°–20°K have been made. The molecule CH_3D exhibits a fine structure at 6.5°K with time-dependent intensities. The data are interpreted in terms of nuclear-spin-species conversion. Because of rapid reconversion at 20°K it is concluded that CH_3D cannot be obtained at room temperature with a nonequilibrium distribution of spin isomers by low-temperature equilibration. The time dependence of the fine structure of the H_2O bending mode at 6.5°K has been reinvestigated. The essence of the previous work is confirmed. The rate of nuclear-spin conversion is found to be rapid at 30°K. The fine structure of the NH_3 umbrella motion exhibits a time dependence which indicates that most of the fine structure observed is not due to rotation.

INTRODUCTION

Since the discovery of ortho- and parahydrogen by Giauque and Johnston,[1] the phenomenon of nuclear-spin-species conversion has been of considerable interest. It has been possible to prepare separated isomers in the gas phase at room temperature only for H_2, D_2, and T_2. There is a considerable body of theory and experimental results for these molecules.[2] However, it is of interest to consider other molecules.

Ideally spin-species conversion should be studied in the gas phase because the nature of the energy levels is well understood and it is easiest to develop a theory[3] of the conversion process for the gas phase. However, it has not been possible to prepare a nonequilibrium distribution except for the hydrogen isotopes mentioned above.

The infrared bands of several hydride molecules isolated in rare-gas matrices at low temperature have been observed to exhibit a fine structure. This fine structure is often interpreted as arising from some form of hindered rotation of the molecule in the matrix cage. The nuclear-spin-species conversion in the matrix may be studied by following the intensity changes of the fine-structure components. The first attempt to do this was by Glasel[4] who studied H_2O at 20°K, but he was not able to conclude that he had actually observed conversion. Redington and Milligan[5] studied the time dependence of the fine structure of the infrared bands of H_2O at 5°K. They observed intensity changes occurring over about 3 h. The process was catalyzed by O_2. Redington and Milligan[5] were able to assign rotational quantum numbers for many of the observed lines. The results clearly indicated that nuclear-spin-species conversion was observed. Recently CH_4 has been carefully

* This work was supported by the Robert A. Welch Foundation Grants C-071 and C-092, by the Atomic Energy Commission, and by National Science Foundation Grant GP 6305X.

† Present address: Department of Chemistry, Georgia State College, Atlanta, Ga.

[1] W. F. Giauque and H. L. Johnston, J. Am. Chem. Soc. **50**, 3221 (1928).

[2] A. Farkas, *Orthohydrogen, Parahydrogen, and Heavy Hydrogen* (Cambridge University Press, Cambridge, England, 1935).

[3] R. F. Curl, J. V. V. Kasper, and K. S. Pitzer, J. Chem. Phys. **46**, 3220 (1967).

[4] J. A. Glasel, J. Chem. Phys. **33**, 252 (1960).

[5] R. L. Redington and D. E. Milligan, J. Chem. Phys. **39**, 1276 (1963).